Pharmacophore

ISSN-2229-5402

Journal home page: http://www.pharmacophorejournal.com

EFFECT OF 3D IMPURITIES OF TRANSITION METALS ON THE ELECTRONIC STRUCTURE OF ANATASE AND RUTILE PHASES IN TIO2

S.M. Esfandfard

University of Applied Science and Technology, Tehran, Iran

ARTICLE INFO

Received:
03th Jun 2017
Accepted:
29th Nov 2017
Available online:
14th Dec 2017

Keywords: *TiO2-based photocatalysts; anatase and rutile; oxygen deficiency; 3d intermediates.*

ABSTRACT

In this work, The influential parameters on photocatalytic activity of titania, more specifically anatase to rutile transformation and electronic structure in response to substitution of Ti with 3 d of transition metals have been investigated. The systematic computations of the formation and stability of crystalline energy of TiO2 anatase and rutile doped to intermediates 3d are performed using FHI-aims, a package based on the developed density functional theory. From the scrutiny of energy calculations of structures that were doped with 3d intermediates, it was found that all 3d impurities rutile were stable over the anatase phase, which determined the rutile stabilization strength in such systems as Co> Zn> Cu> Sc> Ni > Mn> Cr> Fe> V. This agent can reduce the percentage of anatase in the titanium compound and lead to lower activity. Electronic structure's calculations show that V, Cr, Mn, Fe, Co and Ni dopants can cause photocatalytic activity in visible range by creation of defect levels in band gap. Partial density of state (pDOS) of titania showed that the d(Ti) and p(O) states have the main contribution of conduction band (CB) minimum and valance band (VB) maximum respectively. Presence of V impurity creates the defect sates in bottom of the conduction band giving rise a red shift in the gap. In case of Sc, Cu and Zn, the defect states of impurities aren't seen in the gap.

To Cite This Article: S.M. Esfandfard (2017), "Effect of 3d Impurities of Transition Metals on the Electronic Structure of Anatase and Rutile Phases in TiO2", ***Pharmacophore, 8(6S),***e-1173835.

Introduction

Titanium dioxide (titania) has attracted a great deal of attention in different industrial fields such as renewable energy, self-cleaning, and pollutant removal due to its low price, amphoteric nature, and biocompatibility [1-10]. Owing to the energy levels of valence and conduction bands and their capacity, titania is introduced as a high-performance photocatalyst, capable of producing hydrogen out of water splitting process (solar hydrogen) and oxidizing different organic molecules in response to sunlight [11-16]. As with other semi-conductor photocatalysts, titania facilitates reactions from production of electron-hole pairs (excitons) through radiation beyond semiconductor energy gap.

Titania has two main phases, rutile phase which is stable thermodynamically, and anatase phase which is pseudo-stable and converted to rutile by increasing heat [17, 18]. Previous studies have revealed that anatase is a better photocatalyst than rutile due to its indirect band gap (low recombination) and higher specific surface area [19-22]. However, its main deficiency is high band gap (3.2 eV), which covers only a small region of sunlight [23-25]. Two main approaches for this problem involve increasing O-vacancy concentration and/or substituting Ti by other cations [26-60]. O-vacancy and Ti-substitution introduce band gap engineering by locating some new bends in the forbidden region of the band gap [61-66]. Both processes bring about the following effects: the band gap declines; charge separation and thus electron-hole recombination rate diminish; introduction of medium gap state; the oxygen vacancies react in the reaction as active surface centers [67, 68].

Experiments have shown that anatse to rutile can be prevented through substitution of cations with a high charge density [69-73]. However, this is not a general rule, and a cation with a high charge density can enhance anatase to rutile phase transformation. Therefore, the details of mechanism of reducing or enhancing anatse to rutile phase transformation are an open challenging question [74, 75].

Generally, doping and oxygen vacancy both can affect the crystalline and electronic structures and in turn the system

Corresponding Author: S.M. Esfandfard, University of Applied Science and Technology, Tehran, Iran

performance [76, 77]. Two electrons leaving from O-vacancy can occupy Ti levels whose energy reduction is associated with decreased conduction band energy. On the other hand, use of action in substitutional or interstitial form introduces a new band in the band gap region.

although many studies have been carried out on the TiO2-doped metal intermediates experimentally and theoretically However, there are contradictory results on the effect of these collecting metals on their mechanism of action. Since the superiority of the anatase phase performance relative to the rutile, as well as the positive effect of the presence of deficiency of oxygen, has been confirmed. Investigating the effect of third row (3d) mediating metals on anatase stability versus rutile and energy of formation of oxygen deficiency by calculation method The density functional theory has been paid. Understanding the transformation of anatase to rutile fuzzy problem is a very important issue because it is possible to study the activity of photocatalytic activity or other applications of TiO2. The composition of the phase of matter is an important subject affecting their properties and performance, and thus, it is desirable to improve or inhibit the fuzzy transform reaction, in order to prepare the desired phase. Also, the results of the electronic structures provide the ability to predict the exciting energy to create electron-hole pair and then the photocatalytic activity.

2. Calculation details

Full-potential FHI-aims program has been used for all calculations [78, 79]. The revised form of Pardew, Burke, and Ernzerh (rPBE) level of theory was used to optimize bulk of the pure and doped supercells of rutile and anatase phases of TiO_2 [80]. Scalar ZORA approach has been considered to increase correctness of calculations. The criteria for convergence of energy, density and force were set to 5×10^{-6}eV , 5×10^{-5}eV and 0.2 $^{eV}/_{A^{\circ}}$, respectively [81, 82].

4×4×6 and 6×6×2 k-grids have been used to model the first brillouin zone for rutile and anatase unit cells, respectively. 2×2×1 and 2×2×2 supercells for anatase and rutile have been used to study effect of doped cations (Fig. 1). Rutile and anatase supercells contain 48 atoms which are 12 Ti + 36 O. The concentration of cations is equal to 6.25% at. Also, in all calculation O-vacancy concentration was set to be 3.125% at. (only one oxygen atom has been removed from the supercell,). Then, concurrent with dopants and oxygen defect, by investigating all different states, we found the most stable site for developing oxygen defect in the anatase and rutile structures in the presence of impurity. Fig. 2 reveals the most stable form.

In this paper, we have studied the effect of O-vacancy and dopant on the model, simultaneously. To study the effects of O-vacancy and dopant, pDOS and band structure of all supercells have been calculated. For band structure, Γ (0.0 0.00.0) -X (0.0 0.5 0.5) -Γ-Z (0.5 0.5 -0.5) -N (0.0 0.5 0.0) -P (0.25 0.25 0.25) -Z -X -P directions have been considered. k-gird for all DOS calculations was set to 12×12×27 and 27×27×12 for rutile and anatse, respectively.

3. Results & Discussion

3.1 unit cell

Experimental cell parameters for rutile (r-TiO_2) are a = 4.594 Å and c = 2.959 Å and for anatase (a-TiO_2), these parameters are a = 3.784 Å, c = 9.514 Å [83]. Our pbe calculation results for rutile were a = 4.57 Å and c = 2.94 Å, and for anatase were a = 3.75 Å and c = 9.6 Å. After structural relaxation, electronic properties of anatase and rutile phase of titania were analyzed. Fig. 3 illustrates DOS and band structure in which anatase and rutile phases had a band gap energy of 2.13 and 1.8 eV. These values are lower than the experimental values (3 and 3.2 eV for anatase and rutile, respectively) which are due to intrinsic limitation of DFT calculations. However, DFT calculations can precisely predict the relative energy gap which was the aim of this study as well. Also, pDOS calculation analysis indicated that for both anatase and rutile phases, oxygen p-orbitals and titanium d-orbitals have a major contribution to the upper edge of the valence band and the lower edge of the conduction band, respectively (Fig. 3, 8).

In this work, ΔE was defined as E(r-TiO_2) −E(a-TiO_2), representing the extent of phase stability in TiO_2. Positive ΔE suggests that energetically, a-TiO_2 is more desirable than r-TiO_2. DFT calculations indicated that a-TiO_2 is more stable than r-TiO_2 by 1.65 eV for the 48-atom supercell, which is in line with the previous theoretical findings [84, 85]. However, it has been reported that such a small stability limit, given the crystal growth conditions and presence of impurities, makes a-TiO_2 stabilization impossible, and thus phase transformation from a-TiO_2 to r-TiO_2 becomes irreversible [86].

3.2 doped TiO_2

Impurity (Im) atoms have been connected to six adjacent O atoms, forming a body-centered octahedral for $Im_1Ti_{15}O_{32}$ systems. However, in Im1Ti15O31 systems, they are connected to five O atoms. The cell parameters of anatase and rutile supercells have been calculated for all doped TiO2. For pure TiO2, the constants of the supercell a, c are 7.564, 9.564 Å in anatase, and 9.210, 5.920 Å in rutile, respectively. On the other hand, these values change in Im1Ti15O32 systems. As expected from the ionic radius, impurities can increase the cell volume in anatase and rutile phase. Table 1 indicates the parameters of pure and doped anatase and rutile cells. Fig. 3 shows changing of the cell volume versus the capacity of the impurities.

To investigate the effect of impurities on relative stability of a-TiO2 on r-TiO2, the structural ground state energy of TiO2 doped with different impurities was calculated in both a-TiO2 and r-TiO2 systems [87].

Table 2 and fig. 4 show shows the comparison of the anatase and rutile stability with the effect of cationic infiltration of 3d elemental elements. The results indicate that the replacement of 3d impurity atoms instead of Ti reduces the relative stability of anatase to rutile and accelerates the transformation of anatase to rutile, which reduces the effect of Titanium photocatalysis

in this way. Among the cations, vanadium and iron, the lowest (about 0.2 eV) and cobalt and zinc have the highest (by about 0.9 electron volts) effect on the reduction of the relative stability of anatase to rutile.
The pDOS calculation analysis (Fig. 4, 5, 9, 10) shows that unlike the 3d elements that cause the defect states in the gap [109,110]. The electronic structure of doped Titania was investigated. As the calculations revealed, Mn, Cr and Ni significantly increased the gap in both phases in which Mn induced the highest increase among the dopants. Moreover, Zn,Co,V and Fe had highest impact in reducing the gap . However, this impact is not that much to cause the significant activity in visible range. In addition, among the dopants, Zn and Co managed to create defect levels inside the gap which will result in photocatalytic activities in visible range.

3.3. Electronic structure

When a Ti atom is replaced with 3d impurities of Sc, V, Cr, Mn, Fe, Co, Ni, Cu or Zn atom, the states of the dopants shift to a lower energy where the energies of these states become lower and lower. Figs. 5, 6 show pDOS of 3d-doped anatase and rutile respectively. Here, when Ti atom was replace with Sc atom, Sc 3d states are higher than Ti 3d states in the conduction band. V 3d states and Ti 3d states are very close which create the defect states in bottom of the CB. This trend is seen when the atomic number of the impurities increased where with Cr, Mn, Fe, Co and Ni more states are introduced into the band gap and after that for Cu and Zn these states located under the VB. So, only V, Cr, Mn, Fe, Co and Ni conclude the defect states inside the band gap giving rise a photocatalytic activity in the visible light region.
On the other hand, analysis of pDOS of 3d-doped anatase and rutile show that the defect states in the ban gap contain the 3d states of the impurities mainly. It shows the localized properties of the defect states inside the band gap due to the substituted 3d dopants. According to the crystal field theory these states is mainly 3dxy of impurity atoms.

4. Conclusion

Theoretical investigations based on the density functional function theory using a complete potential approach to the anatase and rutile (titanium) structures with impurities 3d (Sc, V, Cr, Mn, Fe, Co, Ni, Cu, Zn) Substituting Ti atom in the structure were done. Studies have shown that all impurities in an intact crystalline structure facilitate the transformation of anatase to rutile, which in turn reduces the active phase of photocatalytic anatase in the total combined composition and can lead to reduced activity. Electronic structure of doped TiO2 showed that only V, Cr, Mn, Fe, Co and Ni dopants can cause photocatalytic activity in visible range by creation of defect levels in band gap.

5. References

1. E. Souteynard, D. Nicolas, J.R. Martin, Semiconductor/metal/gas behaviour through surface-potential change, J.Sens. Act. Chem. 25 (1995) 871-875.
2. A. Fujishima, Electrochemical photolysis of water at a semiconductor electrode, J. Nature. 238 (1972) 37-38.
3. M.R. Elahifard, S. Rahimnejad, S. Haghighi, M.R. Gholami, Apatite-Coated Ag/AgBr/TiO_2 Visible-Light Photocatalyst for Destruction of Bacteria, J. Am. Chem. Soc, 129 (2007) 9552-9553.
4. M. Azimzadehirani, M.R. Elahifard, S. Haghighi, M.R.Gholami, Highly efficient hydroxyapatite/TiO_2 composites covered by silver halides as E. coli disinfectant under visible light and dark media, J. Photochem. Photobiol. Sci. 12 (2013)1787-1794.
5. E. Souteynard, D. Nicolas J. R. Martin, Semiconductor/metal/gas behaviour through surface-potential change, Sens. Act. Chem. 25 (1995) 871-875.
6. N. Mohaghegh, S. Kamrani, M. Tasviri, M.R. Elahifard, M.R. Gholami, Nanoporous Ag_2O photocatalysts based on copper terephthalate metal–organic frameworks, J. Mater. Sci. 50 (2015) 4536-4546.
7. M.R. Elahifard, M. Padervand, S.Yasini, E. Fazeli, The effect of double impurity cluster of Ni and Co in TiO_2 bulk; a DFT study, J. Elec. 37 (2016)4536-4544.
8. A. Kiani- Karanji, M. Padervand, M.R. Elahifard, Copper, Gold, and Silver Decorated Magnetic Core-polymeric Shell Nanostructures for Destruction of Pathogenic Bacteria, J.Phys.Chem. 91 (2017)936-945.
9. M.R. Elahifard, R. VatanMeidanshahi, Photo-deposition of Ag metal particles on Ni-doped TiO_2 for photocatalytic application, Prog. React. Kinet. Mech. 42(2017) 244-250.
10. M.R. Elahifard, M.R. Gholami, Acid blue 92 photocatalytic degradation in the presence of scavengers by two types photocatalyst, Environ. Prog.Sus.Energy. 31(2012) 371-378.
11. S.C. Padmanabhan, S.C. Pillai, J. Colreavy, S. Balakrishnan, D. E. McCormack, T. S. Perova, S. J. Hinder, J. M. Kelly, A simple sol-gel processing for the development of high-temperature stable photoactive anatasetitania, J.Chem. Mater. 19 (2007) 4474-4481.
12. O. Carp, C.L. Huisman, A. Reller, Photoinduced reactivity of titanium dioxide, Prog. Solid State Chem. 32 (2004) 33-177.
13. S. S. Madaeni, N. Ghaemi, Characterization of self-cleaning RO membranes coated with TiO_2 particles under UV irradiation, J.Membrane. Sci. 303 (2007) 221-233.

14. A. Zhang, S. Yan-Ping, Photocatalytic killing effect of TiO_2 nanoparticles on Ls-174-t human colon carcinoma cells, World J. Gastroenterol.10 (2004) 3191-3193.
15. P. Biju, K. Mahaveer, Effect of crystallization on humidity sensing properties of sol–gel derived nanocrystalline TiO2 thin films, J. Solid Films 516 (2008) 2175-2180.
16. R. Xie, S. Jian-Ku, W. Pinggui, Quaternary oxides and catalysts containing quaternary oxides, U.S. Patent No. 8, 541, 337. 24 Sep. (2013).
17. S. Mahshid, M. Askari, M. Sasani-Ghamsari, Synthesis of TiO_2 nanoparticles by hydrolysis and peptization of titanium isopropoxide solution, J. Phys. Quantum. Elec. Optoelec. 9 (2006) 658-663.
18. W. Choi, T. Andreas, R.M. Hoffmann, The role of metal ion dopants in quantum-sized TiO_2: correlation between photoreactivity and charge carrier recombination dynamics, J. Phys. Chem. 98 (1994) 13669-13679.
19. S. Pillai, S.C. Pillai, P. Periyat, R. George, D.E. McCormack, M.K. Seery, H. Hayden, J. Colreavy, D. Corr, S.J. Hinder, Synthesis of high-temperature stable anatase TiO_2 photocatalyst, J. Phys. Chem. C. 111 (2007) 1605-1611.
20. E. Poulsen, A. James, Extractive metallurgy of titanium: a review of the state of the art and evolving production techniques, JOM. 35 (1983) 60-65.
21. U. Diebold, The surface science of titanium dioxide, J. Sci. Rep. 48 (2003) 53-229.
22. C.S. Enache, Characterization of Thin Film Photoanodesfor Solar Water Splitting, University of Transilvania, PhD Thesis (2012).
23. A. Kudo, M. Yugo, Heterogeneous photocatalyst materials for water splitting, J. Chem. Soc. Rev. 38 (2009) 253-278.
24. A. Fujishima,T.N. Rao, D.A. Tryk, Titanium dioxide photocatalysis, J. Photochem. Photobiol. Rev. 1 (2000) 1-21.
25. A.L. Linsebigler, G. Lu, J.T. Yates, Photocatalysis on TiO_2 surfaces: principles, mechanisms, and selected results, J. Chem. Rrev. 95 (1995) 735-758.
26. S. Sato, R. Nakamura, S. Abe, Visible-light sensitization of TiO_2 photocatalysts by wet-method N dopingAppl, J. Catal. A. 284 (2005) 131-137.
27. M. Padervand, M.R. Elahifard, R. VatanMeidanshahi, S. Ghasemi, S. Haghighi, M.R. Gholami, Investigation of the antibacterial and photocatalytic properties of the zeolitic nanosized $AgBr/TiO_2$ composites, Mater. Sci. Semicond. Process. 15 (2102) 73-79.
28. J.C. Yu, J.Ho. Yu, Effects of F-Doping on the Photocatalytic Activity and Microstructures of Nanocrystalline TiO2Powders, J. Chem. Mater. 14 (2002) 3808-3816.
29. T. Umebayashi, T. Yamaki, S. Yamamoto, A. Miyashita, S. Tanaka, T.K. Sumita, Sulfur-doping of rutile-titanium dioxide by ion implantation: Photocurrent spectroscopy and first-principles band calculation studies, J. Asai. Appl. Phys. 93 (2003) 5156-5160.
30. Y.F. Wang, C.X. Feng, M. Zhang, J. Yang, Z. Zhang, Enhanced visible light photocatalytic activity of N-doped TiO2 in relation to single-electron-trapped oxygen vacancy and doped-nitrogen, J. Appl. Catal. B: Environ. 1 (2010) 84-90.
31. M.R. Elahifard, S. Rahimnejad, R. Pourbaba, S. Haghighi, M.R. Gholami, Photocatalytic mechanism of action of apatite-coated $Ag/AgBr/TiO_2$ on phenol and Escherichia coli and Bacillus subtilis bacteria under various conditions, Prog. React. Kinet. Mech. 36 (2011) 38-52.
32. R.y. Abe, Recent progress on photocatalytic and photoelectrochemical water splitting under visible light irradiation, J. Photochem. Photobiol. C. 11 (2010) 179-209.
33. X. Chen, S.S. Mao, Synthesis, Titanium Dioxide Nanomaterials: Synthesis, Properties, Modifications, and Applications, J. Chem. Inform. 107 (2007) 2891-2959.
34. M.R. Elahifard, S. Ahmadvand, A. Mirzanejad, Effects of Ni-doping on the photo-catalytic activity of TiO2 anatase and rutile: Simulation and experiment, Mater. Sci. Semicond. Process. 84 (2018) 10-16.
35. S. Sakthivel, H. Kisch, Daylight photocatalysis by carbon-modified titanium dioxide, J. Angew, Chem. Int. Ed. 42 (2003) 4908-4911.
36. R. Asahi, T. Morikawa, T. Ohwaki, K. Aoki, Visible-Light Photocatalysis in Nitrogen-Doped Titanium Oxides, J. Sci. 293 (2001) 269-271.
37. H. Park, J. Lee, W. Choi, Study of Special Cases Where the Enhanced Photocatalytic Activities of Pt/TiO2 Vanish Under Low Light Intensity, J. Catal. Today. 111 (2006) 259–265.
38. I.H. Tseng, W.C. Chang, J.C.S. Wu, Photoreduction of CO2 Using Sol–Gel Derived Titania and Titania-Supported Copper Catalysts, Appl. Catal. B. Environ. 37 (2002) 37-48.
39. P.V. Kamat, M. Flumiani, A. Dawson, Metal-Metal and Metal-Semiconductor Composite Nanoclusters, Colloid. Surf. Physicochem. Eng. Aspects. 202 (2002) 269-279.
40. S.M. Esfandfard, M.R. Elahifard, R. Behjatmanesh-Ardakani, H. Kargar, DFT Study on Oxygen-Vacancy Stability in Rutile/Anatase TiO_2: Effect of Cationic Substitutions, Phys. Chem. Res. 6 (2018) 547-563.
41. W.Y. Choi, A. Termin, M.R. Hoffmann, The Role of Metal-Ion Dopants in Quantum- Sized TiO_2: Correlation Between Photoreactivity and Charge-Carrier Recombination Dynamics, J. Phys. Chem. 84 (1994) 13669-13679.

42. A. Hameed, M.A. Gondal, Z.H. Yamani, Effect of Transition Metal Doping on Photocatalytic Activity of WO_3 For Water Splitting Under Laser Illumination: Role of 3d- Orbitals, J. Catal. 5 (2004) 715-719.
43. J. Wade, An investigation of TiO_2-$ZnFe_2O_4$ nanocomposites for visible light photocatalysis, Diss. U. S. F. (2005).
44. A. Kudo, M. Yugo, Heterogeneous photocatalyst materials for water splitting, Chem. Soc. Rev. 38 (2009) 253-278.
45. A. Fujishima, Titanium dioxide photocatalysis, J. Photochem. Photobio. C. 1.1 (2000) 1-21.
46. L. Linsebigler, Photocatalysis on TiO2 surfaces: principles, mechanisms, and selected results, J. Chem. Rev. 95 (1995) 735-758.
47. R. Abe, Recent progress on photocatalytic and photoelectrochemical water splitting under visible light irradiation, J. Photochem. Photobiol. C. 11 (2010) 179-209.
48. J. Tian, N-doped TiO_2/ZnO composite powder and its photocatalytic performance for degradation of methyl orange, Surf. Coat. Technol. 204 (2009) 723-730.
49. U. Diebold, The surface science of titanium dioxide, J. Surf. Sci. Rep. 48 (2003) 53-229.
50. N.L. Wu, M.S. Lee, Enhanced TiO2 Photocatalysis By Cu in Hydrogen Production From Aqueous Methanol Solution, Int. J. Hydr. En. 29 (2004) 1601-1605.
51. W. Chen, P. Yuan, S. Zhang, Q. Sun, E. Liang, Y. Jia, Electronic properties of anatase TiO_2 doped by lanthanides: A DFT+ U study, J. Physica. B: Condensed Matter. 407.6 (2012) 1038-1043.
52. F. Maldonado, R. Rivera, A. Stashans, Structure, electronic and magnetic properties of Ca-doped chromium oxide studied by the DFT method, J. Physica. B: Condensed Matter. 407.8 (2012) 1262-1267.
53. M. Guo, J. Du, First-principles study of electronic structures and optical properties of Cu, Ag, and Au-doped anatase TiO2, J. Physica. B: Condensed Matter. 407.6 (2012) 1003-1007.
54. M.L. Guo, X.D. Zhang, C.T. Liang, Concentration-dependent electronic structure and optical absorption properties of B-doped anatase TiO_2, J. Physica. B: Condensed Matter. 406.17 (2012) 3354-3358.
55. C. Zhang, Y. Jia, Y. Jing, Y. Yao, J. Ma, J. Sun, DFT study on electronic structure and optical properties of N-doped, S-doped, and N/S co-doped $SrTiO_3$, J. Physica. B: Condensed Matter. 407.24 (2012) 4649-4654.
56. M.L. Guo, X.D. Zhang, C.T. Liang, Concentration-dependent electronic structure and optical absorption properties of B-doped anatase TiO2, J. Physica. B: Condensed Matter. 406.17 (2011) 3354-3358.
57. Q. Chen, C. Tang, G. Zheng, First-principles study of anatase (101) surfaces doped with N, J. Physica. B: Condensed Matter. 404.8 (2009) 1074-1078.
58. C.E. Rodríguez Torres, A.F. Cabrera, M.B. Fernández van Raap, F.H. Sánchez, Mössbauer study of mechanical alloyed Fe-doped TiO2 compounds, J. Physica. B: Condensed Matter. 354.1 (2004) 67-70.
59. K.C. Zhang, Y.F. Li, Y. Liu, Y. Zhu, Possible ferromagnetism in Cd-doped TiO_2: A first-principles study, J. Physica. B: Condensed Matter. 422 (2013) 28-32.
60. A.F. Cabrera, C.E. Rodríguez Torres, L. Errico, F.H. Sánchez, Study of Fe-doped rutile TiO_2 alloys obtained by mechanical alloying, J. Physica. B: Condensed Matter. 384.1 (2006) 345-347.
61. V. Ranki, K. Saarinen, Formation of vacancy-impurity complexes in highly As- and P-doped Si, J. Physica. B: Condensed Matter. 340 (2003) 765-768.
62. B. Zhang, Y. Tian, J.X. Zhang, W. Cai, The role of oxygen vacancy in fluorine-doped SnO_2 films, J. Physica. B: Condensed Matter. 406.9 (2011) 1822-1826.
63. B. Almquist, B. Pratim, Role of Synthesis Method and Particle Size of Nanostructured TiO_2 on Its Photoactivity, J. Catal. 212 (2002) 145-156.
64. N. Serpone, Is the Band Gap of Pristine TiO2 Narrowed by Anion- and Cation-Doping of Titanium Dioxide in Second-Generation Photocatalysts?, J. Phys. Chem. B. 110 (2006) 24287-24293.
65. K.T. Ranjit, H. Cohen, I. Willner, S. Bossmann, A.M. Braun, Lanthanide oxide-doped titanium dioxide: Effective photocatalysts for the degradation of organic pollutants, J. Mater. Sci. 34(1999)5273-5280.
66. K. Nagaveni, M.S. Hegde, N. Ravishankar, G.N. Subbanna, G. Madrass, Synthesis and structure of nanocrystalline TiO2 with lower band gap showing high photocatalytic activity, J. Langmuir. 20(2004) 2900-2907.
67. W. Chen, S. Samuel, Titanium dioxide nanomaterials: synthesis, properties, modifications, and applications, J. Chem. Rev. 107 (2007) 2891-2959.
68. L. Hongfei, G. Yuzheng, J. Robertson, Calculation of TiO_2 Surface and Subsurface Oxygen Vacancy by the Screened Exchange Functional, J. Phys. Chem. C. 119 (2015) 18160-18166
69. A.Dorian, H. Hanaor, C. Charles, Review of the anataseto rutile phase transformation, J. Mater Sci. 46 (2011) 855–874.
70. E.F. Heald, C.W. Weiss, Kinetics and mechanism of the anatase/rutile transformation, as catalyzed by ferric oxide and reducing conditions, Am. Miner. 57 (1972) 10-23.
71. R. Janes, L.J. Knightley, C.J. Harding, Structural and spectroscopic studies of iron (III) doped titania powders prepared by sol-gel synthesis and hydrothermal processing, J. Dyes Pig. 62 (2004) 199-212.
72. F.C. Gennari, D.M. Pasquevich, Kinetics of the anatase-rutile transformation in TiO2 in the presence of Fe_2O_3, J. Mater. Sci. 33(1998) 1571-1578.

73. S.A. Borkar, S.R. Dharwadkar, Temperatures and kinetics of anatase to rutile transformation in doped TiO2 heated in microwave field, J. Therm. Anal. Calorim. 78 (2004) 761-767.
74. M.S. Francisco, V.R. Mastelaro, Inhibition of the Anatase-Rutile phase Transformation with Addition of CeO_2 to CuO-TiO_2 System: Raman Spectroscopy, X-ray Diffraction, and Textural Studies, J. Chem. Mater. 14 (2002) 2514-2518.
75. J. Nowotny, T. Bak, L.R. Sheppard, C.C. Sorrell, Pulsed laser deposited TiO2films:co-effect of O2 partial pressure and Nd doping, Adv. Solar. Energy.Annu. Rev. Res. Dev. 17(2007) 169-188.
76. C.Q. Sun, Study of Electric Quadrupole Perturbation at Multiple Probe Sites in Hf- doped Rutile in a Single Perturbed Angular Correlation Measurement, J. Chem. Phys. 108 (2014) 805-817.
77. X.Y. Pan, M.Q. Yang, X.Z. Fu, N. Zhang, Y.J. Xu, Defective TiO2 with oxygen vacancies: synthesis, properties and photocatalytic applications, J. Nanoscale. 9 (2013) 3601-3614.
78. V. Blum, R. Gehrke, F. Hanke, P. Havu, V. Havu, X. Ren, K. Reuter, M. Scheffler, Ab initio molecular simulations with numeric atom-centered orbitals.Comput, J. Phys. Commun. 180 (2009) 2175-2196.
79. J. Perdew, K. Burke, M. Ernzerhof, Generalized gradient approximation made simple, J. Phys. Rev. Lett.77 (1996) 3865-3868.
80. F. Abild-Pedersen, M. Andersson, CO adsorption energies on metals with correction for high coordination adsorption sites–A density functional study, J. Surf. Sci. 601 (2007) 1747-1753.
81. E.V. Lenthe, J. Snijders, E. Baerends, The zero order regular approximation for relativistic effects: The effect of spin–orbit coupling in closed shell molecules, J. Chem. Phys. 105 (1996) 6505-6516.
82. M.D. Segall, R. Shah, C.J. Pickard, Population analysis of plane-wave electronic structure calculations of bulk materials, J, Phys. Rev. B. 54 (1996) 16317-16320.
83. D.T. Cromer, K. Herrington, The structures of anatase and rutile. J. Am. Chem. Soc. 77 (1955) 4708–4709.
84. L.A. Curtiss, J.E. Carpenter, K. Raghavachari, Pople JA Validity of additivityapproxiamations in Gaussian theory, J. Chem. Phys. 96 (1992) 9030–9034.
85. D.T. Cromer, K. Herrington, The structures of anatase and rutile, J. Am. Chem. Soc. 77 (1955) 4708–4709.
86. A. Dorian, H. Hanaor, H. Mohammed, N. Assadi, Li. Sean, Yu. Aibing, C. Charles, Ab initio study of phase stability in doped TiO2, J. Comput. Mech. 50 (2012) 185–194.
87. S. Na-Phattalung, M.F. Smith, K. Kim, M.H. Du, S.H. Wei, S.B. Zhang, Limpijumnong S. First-principles study of native defects in anatase TiO2, J. Phys. Rev.73 (2006) 125205-125211.
88. W. Tai, O. Jae-Hee, Fabrication and humidity sensing properties of nanostructured TiO2–SnO2, J. Chem. 85 (2002) 154-157.
89. S. I Shah,W. Li, C.P. Huang, O. Jung, C. Ni, Study of Nd^{3+}, Pd^{2+}, Pt^{4+}, and Fe^{3+} dopant effect on photoreactivity of TiO2 nanoparticles, Proc. Nati. Acad. Sci. Uni. Stat. Am. 99 (2002) 6482-6486.
90. S. John, Hydrogen generation by photocatalytic oxidation of glucose by platinized n-titania powder, J. Phys. Chem. 87 (1983) 801-805.
91. S. Vargas, R. Arroyo, E. Haro, R. Rodriguez, Effects of cationic dopants on the phase transition temperature of titaniaprepared by the sol-gel method, J. Mater. Res1. 4 (1999) 3932-3937.
92. S. Hishita, I. Mutoh, Inhibition mechanism of the anatase-rutile phase transformation by rare earth oxides, J. Ceram Int. 9 (1983) 61-67.
93. J. Yang, J.M.F. Fereira, On the Titania Phase Transition by Zirconia Additive in a Sol-Gel-Derived Powder, Mater. Res. Bull. 33 (1998) 389-394.
94. J. Kim, K.C. Song, S. Foncillas, S. Pratsinis, Dopants for Synthesis of Stable Bimodally Porous Titania, J. Eur. Ceram. Soc. 21(2001) 2863-2872.
95. M. Hirano, N. Nakahara, K. Ota, O. Tanaike, N. Inagaki, Photoactivity and phase stability of ZrO2-doped anatase-type TiO2 directly formed as nanometer-sized particles by hydrolysis under hydrothermal conditions, J. Solid .State. Chem.170 (2003) 39-47.
96. A. Jaroenworaluck, W. Sunsan, R. Stevens, Surface characteristics of zirconia coated TiO2 and its phase transformation, Key. Eng. Mater.1 (2007) 334–335, 1101–1104
97. S. Karvinen, Trace Elements on the Crystal Properties of TiO_2, J. Solids. State. Sci. 5 (2003) 811-819.
98. Z.M. Shi, L.Yan, L.N. Jin, X.M. Lu, G. Zhao, The phase transformation behaviors of Sn^{2+}-doped Titania gels, J. Non-Cryst. Solids. 353 (2007) 2171-2178.
99. M.A. Debeila, M.C. Raphulu, E. Mokoena, M. Avalos, V. Petranovskii, N.J. Coville, M.S. Scurrell, The effect of gold on the phase transitions of titania, Mater. Sci. Eng. A. 396 (2005) 61-69.
100. L.A. Curtiss, J.E. Carpenter, K. Raghavachari, Pople JA Validity of additivityapproxiamations in Gaussian theory, J. Chem. Phys. 96 (1992) 9030–9034
101. A.V. Janotti, P. Rinke, N. Umezawa, G. Kresse, C.G. VandeWalle, Hybrid functional studies of the oxygen vacancy inTiO2, J. Phys. Rev. B. 8 (2010) 085212-085218.

102. J.L. He, E.D. Wu, H.T. Wang, R.P. Liu, Y.J. Tian, Ionicities of Boron-Boron Bonds inB12Icosahedra, J. Phys. Rev. Lett. 94 (2005) 15504-15509.
103. J.C. Phillips, Ionicity of the Chemical Bond in Crystals, Rev. Mod. Phys. 42 (1970) 317-356.
104. K.J. Mackenzie,Kinetics and mechanism of the Mackenzie, Trans. J. Br. Ceram. Soc. 74 (1975) 77-84.
105. K.J. MacKenzie, The effect of additives on the Mackenzie,Trans. J. Br. Ceram. Soc. 74 (1975) 29-34.
106. K.N. Kumar, D.J. Fray, J. Nair, F. Mizukami, T. Okubu, Enhanced anatase-to-rutile phase transformation without exaggerated particle growth in nanostructured titania–tin oxide composites, J. Scripta. Mater. 57 (2007) 771-774.
107. S.J. Smith, R. Stevens, S. Liu, G. Li, A. Navrotsky, J. Boerio-Goates, B.F. Woodfield, Heat capacities and thermodynamic functions of TiO_2 anatase and rutile: analysis of phase stability. Am. Mineral. 94 (2009) 236-243.
108. H. Zhang, J.F. Banfield, Thermodynamic analysis of phase stability of nanocrystalline titania. J. Mater. Chem. 8 (1998) 2073–2076.

Table 1. supercell volume of pure and doped anatase and rutile TiO_2.

System (structure)	Supercell volume in anatase phase	Supercell volume in rutile phase	Percent change in volume in the anatase phase	Percentage change in volume in the rutile phase
pureTiO_2	5.75	5.25	0	0
Sc/TiO_2	5.82	5.30	1.2	0.95
V/TiO_2	5.75	5.23	0	-0.38
Cr/TiO_2	5.72	5.38	-0.52	2.48
Mn/TiO_2	5.72	5.21	-0.52	-0.76
Fe/TiO_2	5.75	5.20	0	-0.95
Co/TiO_2	5.76	5.36	0.17	2.09
Ni/TiO_2	5.71	5.35	-0.70	1.90
Cu/TiO_2	5.76	5.25	0.17	0
Zn/TiO_2	5.81	5.30	1.04	0.95

Table 2. Comparing anatase and rutile stability in response to cationic doping. Atomic and ionic radius are presented too.

dopants	Ti	Sc	V	Cr	Mn	Fe	Co	Ni	Cu	Zn
Relative anatase stability vs rutile (eV)	1.65	1.20	1.49	1.41	1.37	1.48	0.80	1.27	1.40	0.74
Atomic radius (A°)	1.45	1.61	1.32	1.25	1.24	1.24	1.25	1.25	1.28	1.33
Ionic radius (A°)	0.68	0.81	0.52	0.52	0.46	0.64	0.74	0.72	0.72	0.74
capacity	+4	+3	+5	+6	+7	+3	+2	+2	+2	+2

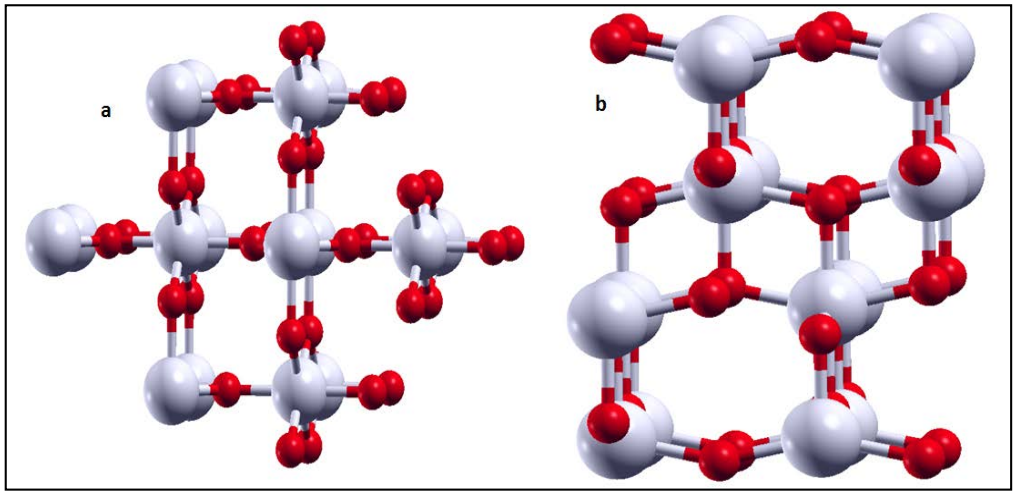

Fig. 1. The crystalline structure of the computational model of 2×2×2 and 2×2×1, 48-atom supercell for rutile (a) and anatase (b), titanium atoms are represented by light grey circles, while oxygen atoms are demonstrated by red circles.

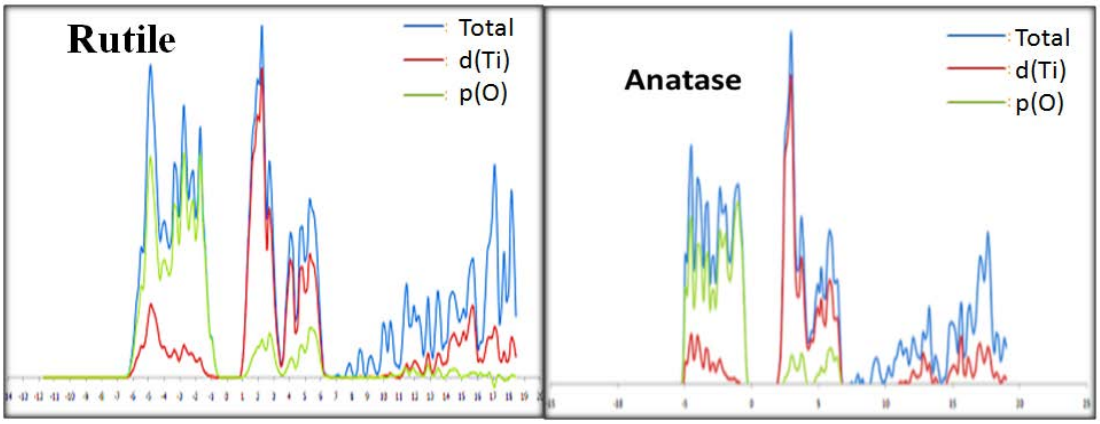

Fig 2. The total and partial DOS of anatase and rutile TiO_2 (Pure) compare with O-vacancy TiO_2.

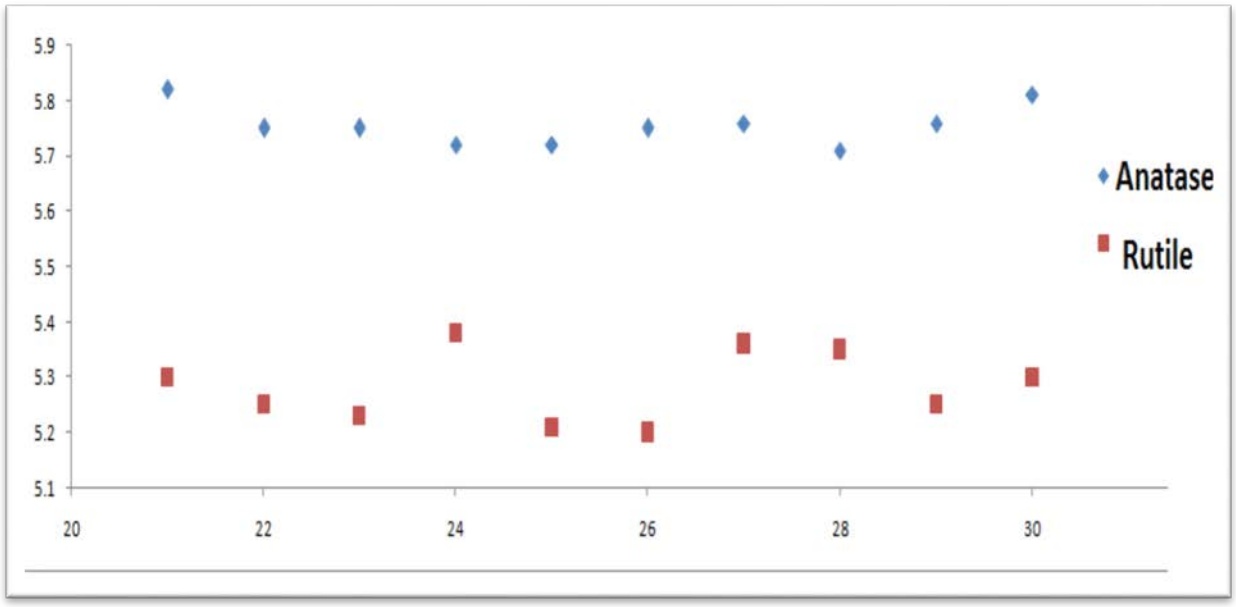

Fig. 3. supercell volume of doped anatase and rutile TiO_2 versus atomic number of impurity.

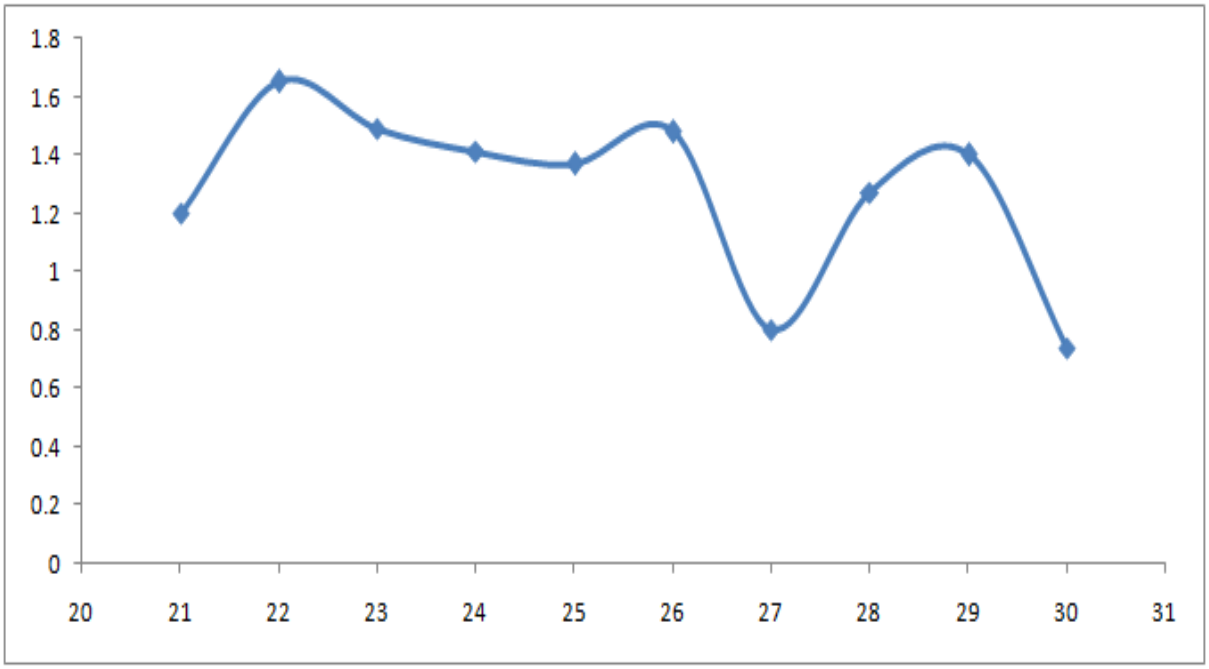

Fig. 4. Comparing anatase and rutile stability in response to atomic number of cationic doping.

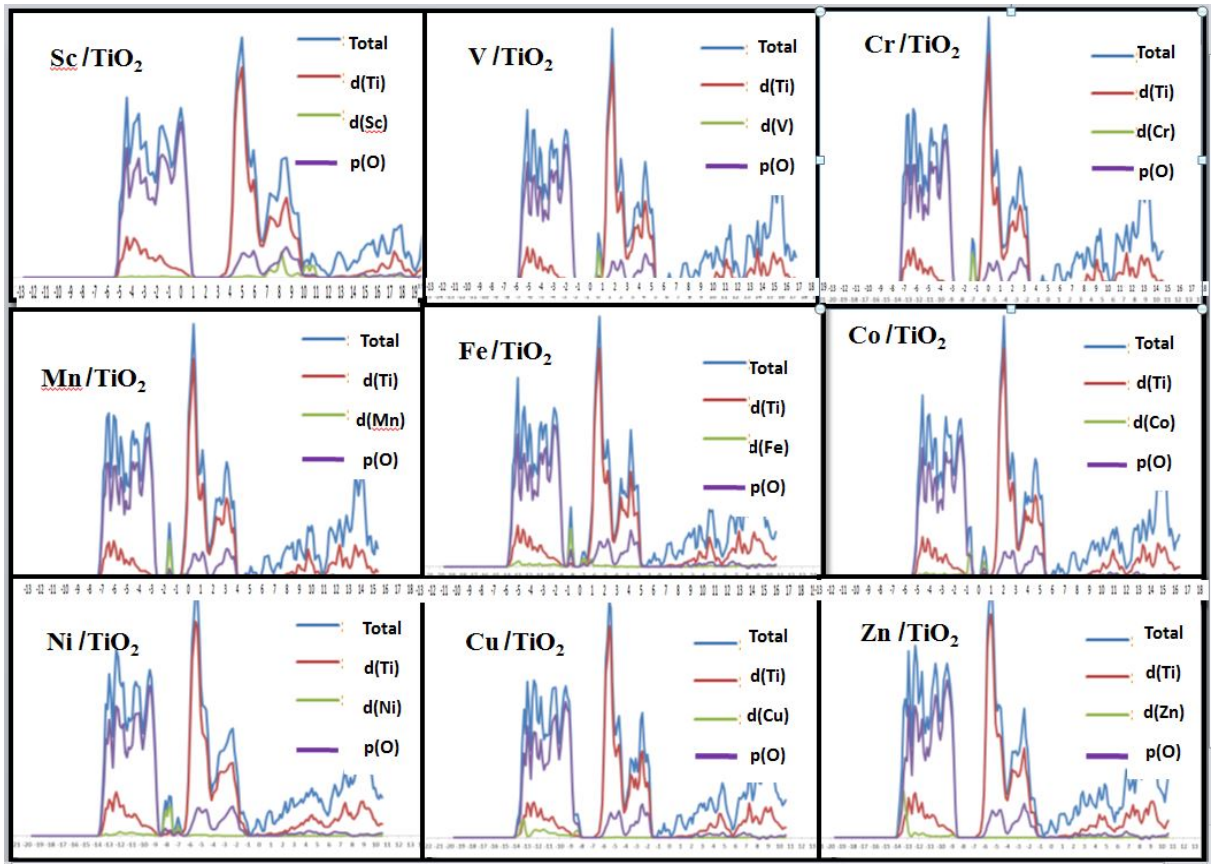

Fig 5. The total and partial DOS of doped anatase TiO_2 compare with Pure TiO_2.

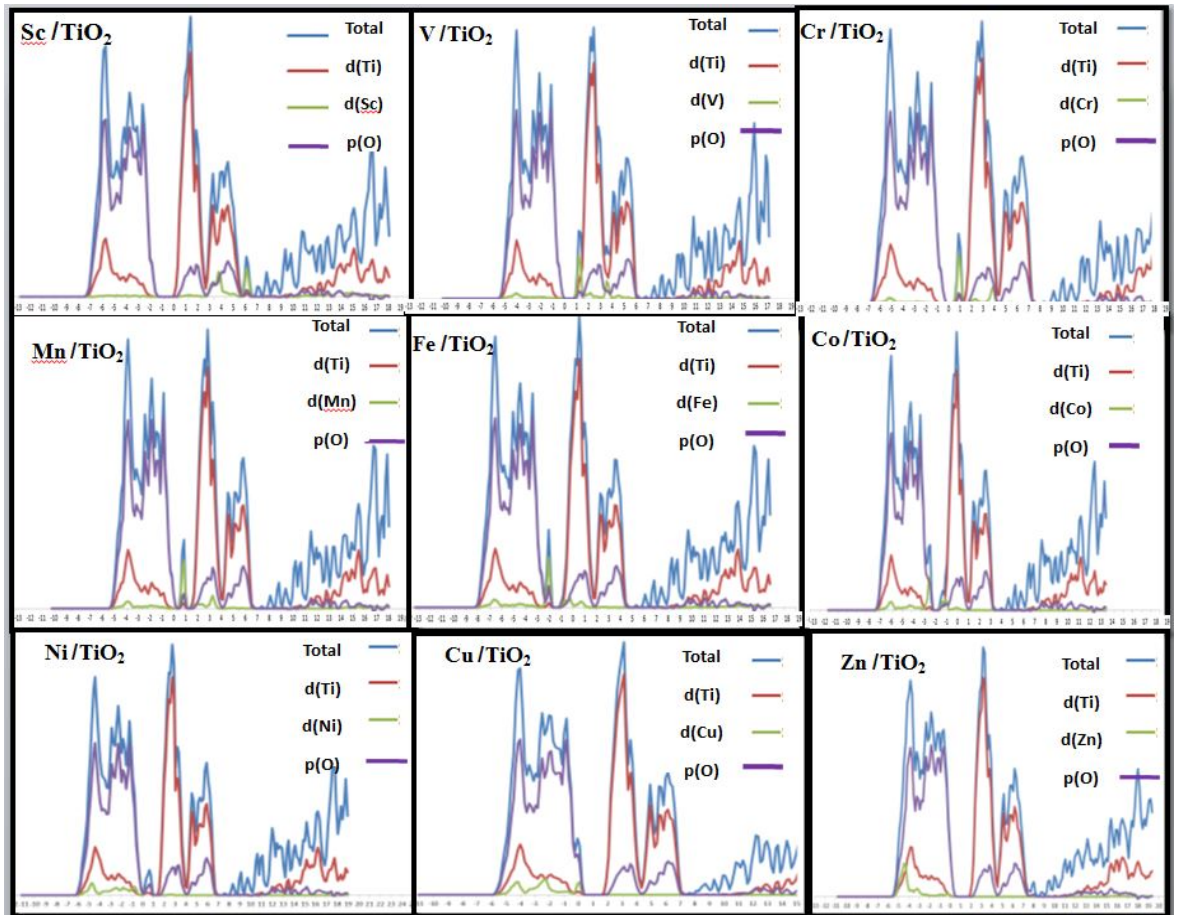

Fig 6. The total and partial DOS of doped rutile TiO_2 compare with Pure TiO_2.